J Technical summary

J.1 Background and scope

The 2D TUFLOW model developed for the 2008 SFRA was updated with new defence and topographical data (Lidar) for this update. In addition, more detailed and up-to-date tidal time series and overtopping rates were calculated, which provide a more accurate representation of the nearshore conditions and the improvements to defences.

J.2 Overtopping calculations and modelling

Over topping modelling was run for the following scenarios

- 0.5% annual exceedance probability (AEP) tide occurrence for
  - current day;
  - climate change (sea level rise) to year 2023;
  - climate change (sea level rise) to year 2055; and
  - climate change (sea level rise) to year 2112.
- 0.1% probability tide occurrence for
  - current day;
  - climate change (sea level rise) to year 2023;
  - climate change (sea level rise) to year 2055; and
  - climate change (sea level rise) to year 2112.

The model simulates three tide cycles with the peak occurring on the second peak.

It is important that the methods used to model coastal processes are as realistic as possible, given the inherent uncertainty many aspects of coastal numerical modelling. In this section the principal mechanisms of coastal flooding by wave overtopping are discussed, providing a conceptual understanding the processes affecting Jaywick.

Figure J-1: Location of study site

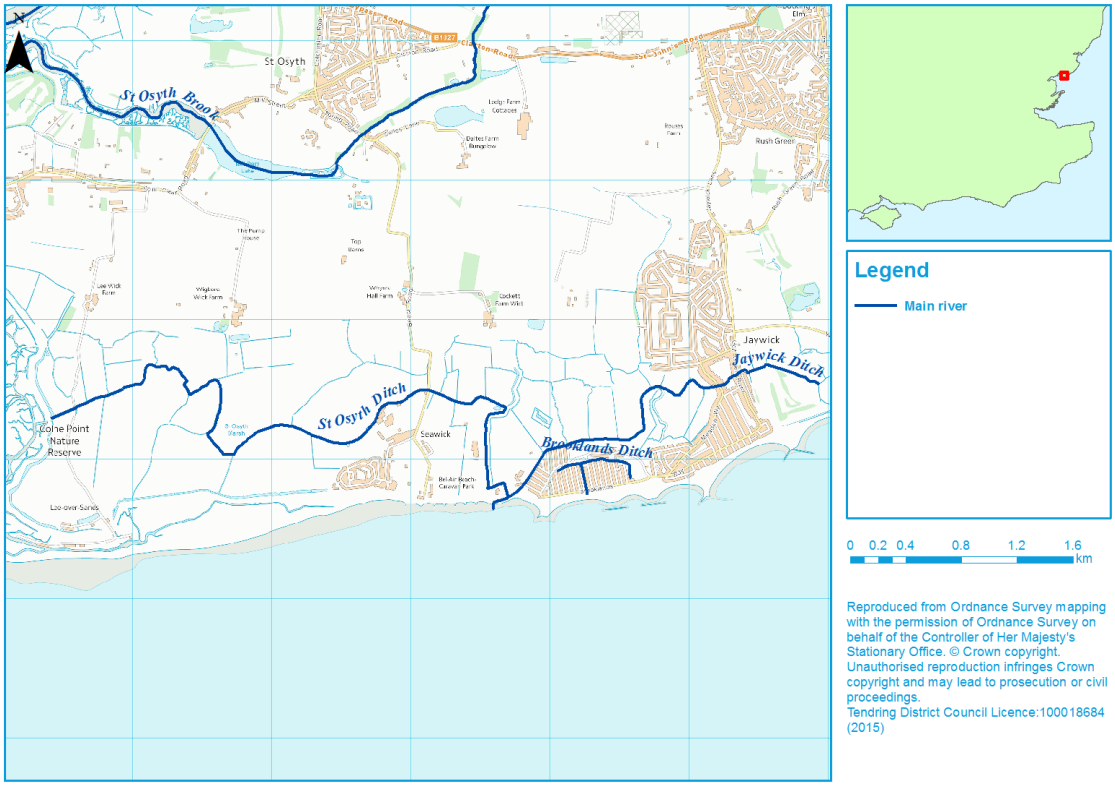

J.2.1 Coastal flood risk drivers

Coastal flooding is a complicated process, affected by a number of dependant and independent variables. Figure J-2 illustrates the main components of sea-level variation that contribute to coastal flooding during a storm event. The base sea-level, often referred to as either the still water sea-level or total sea-level, is comprised of the underlying astronomical tide and the passage of a large scale storm surge. These two components determine the average sea-level for a particular location at a particular time. Whilst this variable is very important in terms of coastal flooding, still water-induced flooding is normally limited to sheltered locations such as ports and harbours. Not surprisingly, the sea is not still during a storm event and for many locations exposed to the sea most flooding occurs through wave action, rather than still water flooding.

Wave action is a complex process controlled by a number of factors. The manner in which these factors combine determines the magnitude of any wave induced flood impacts. Waves generate from wind, typically in deep water and then propagate towards land. As they do so, they enter shallower bathymetry where wave transformation processes occur, including shoaling, diffraction, refraction, depth limitation and breaking. The consequence of these processes is that the properties of the waves, when they reach the base of flood defences, are quite different to the waves in deep water. It is these nearshore waves that are of most importance because they interact with coastal defences and lead to wave overtopping.

Wave overtopping itself is also a complex process controlled by the state of the sea (depth, wave properties), the geometry of the beach and local flood defences. The impact of all of the above flood risk drivers during a particular storm is also heavily dependent upon the location and orientation of the defences with respect to the sea. This means that while one location may be flooded during a storm event another, just a short distance away, may have lesser impacts due to its orientation with respect to the dominant wind/wave direction.

There are two key processes that may lead to coastal flooding at Jaywick; still water flooding or wave overtopping. These two processes can be described considered as follows:

Still Water Level (SWL) flooding occurs where the water level exceeds the defence crest level (commonly the top of the quay/harbour walls) and water inundates the land.

Wave Overtopping occurs where waves run up the face of the coastal defence. Where the wave run-up exceeds the defence crest level, water will pass over the crest and inundate the foreshore.

Figure J-2: Components of sea-level variation that lead to typical coastal flooding

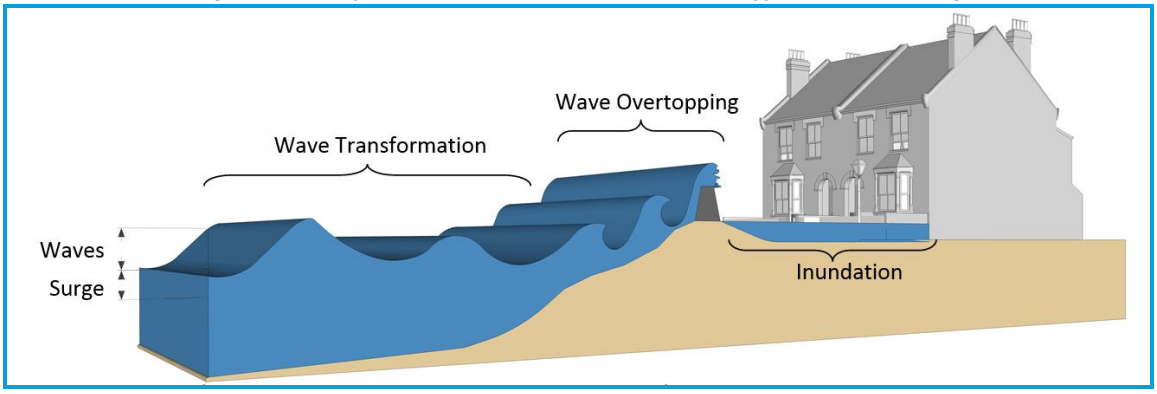

At present there is no one numerical model or calculation approach able to replicate all of these processes. Instead, they are represented through a suite of numerical models as shown in Figure J-3.

Figure J-3: Modelling components of the wave and overtopping modelling

J.3 Modelling flood risk from coastal sources

J.3.2 Introduction

In order to calculate the wave overtopping a number of wave simulations and wave overtopping models were used. First a wave transformation model was used to calculate extreme wave conditions at the toe of the defences. These conditions were then used to calculate the rate of overtopping occurring along the frontage. Each of these elements is described in the following sections.

J.3.3 Wave transformation modelling

Introduction

Wave transformation models simulates how waves develop and change (or 'transform') as they propagate from a deep water location to the toe of defences at the study site. This section details the adapting of the bathymetry of the previously developed North Kent wave transformation model.

Wave model development

All wave scenarios were modelled using the industry-standard SWAN (Simulating WAves Nearshore) model. SWAN is a third generation wave model capable of simulating the following nearshore wave transformation processes:

- Wind-wave interactions, which is the transfer of wind energy into wave energy, leading to the growth of waves
- Shoaling, which is the build-up of energy as a wave enters shallow water, causing an increase in wave height
- Refraction, which is the change in wave speed as waves propagate through areas of changing depth, causing a change in wave direction
- Wave breaking, which is the destabilisation of a wave as it enters shallow water, causing broken waves with the characteristic whitewash or foam on the crest
- Wave dissipation, which limits the size of waves through white-capping, bottom friction and depth-induced breaking

SWAN calculates steady state wave conditions for specific inputs of wave height, period and direction at an offshore boundary, and wind speed and direction applied across the model domain surface. Water levels can also be configured to account for tidal/surge variations.

This project makes use of an existing calibrated SWAN model originally developed for the Environment Agency[20]. Development of the model involved several stages, including construction of a wave model grid, interpolation of a bathymetric dataset, joint probability analysis and extreme event modelling. To ensure accurate wave growth the model domain encompasses the majority of the North Sea, with land boundaries along Kent coastline.

Computational mesh

The model grid, with which SWAN performs its calculations of wave parameters, was designed using an unstructured mesh employing triangular elements. This type of grid allows for very high resolution detail around the complex coastal areas of Jaywick, whilst simultaneously allowing for low resolution across the rest of the open ocean where high resolution detail (which leads to increased computation time) was not required. The mesh resolution varies from 2,935.52m in deep areas of the North Sea to 4.47m in the shallow areas around the near shore structures of Jaywick. This high resolution allows the wave transformation processes to be computed with a

[20]JBA (2013), North Kent Coastal Flood Forecasting System Development

high degree of accuracy, as sudden changes in depth will induce shoaling, diffraction and breaking processes. The wave model comprised 51,152 computational nodes (Figure J-4).

Bathymetry data

A key element of boundary data required for the wave transformation model was a bathymetric dataset representing the elevation of the sea-bed. A bathymetry grid was constructed for the model domain based on several sources of data. For areas of relatively deep water, bathymetry data supplied by SeaZone Solutions Ltd was used. These Seazone data are a composite of "true depth" (surveyed) sources and digitised Admiralty charts. True depth bathymetric data was used extending from the Isle of Grain to the 1˚30'E meridian, and from Ramsgate in the South to Felixstowe in the North. The data are made up from an assortment of surveys that were taken over a period of approximately 12 years from 1995 to 2007. The data are provided on a grid of approximately 20.00m spacing (though this is not necessarily the spacing of the underlying survey points). Seazone Charted Raster bathymetric data has been used where True depth bathymetry were not available. Although these data are of lesser quality than the TruDepths gridded survey data they cover the area of the North Sea that is characterised by deeper depths that will have minimal depth-limitation effects on propagating waves.

Whilst these data provide a good source of bathymetry for deep water locations, higher resolution, more detailed data were supplied for nearshore regions by the Channel Coastal Observatory (CCO). Single beam bathymetric survey data, surveyed during 2006/07, were available for the region extending from Allhallows-on-Sea in the west to Ramsgate in the east. The data were recorded from the nearshore to approximately 1km offshore of the shoreline. LIDAR data has been supplied by the Geomatics Group for the entire coastline of the study area. These data vary in horizontal resolution and coverage, with a varying resolution between 0.25m and 2.00m with the latest data supplied in 2014 including the near shore construction of groynes and off-shore breakwaters and the resulting salients. Topographic survey of sea defence and beach profiles, taken at specific sites along the coastline, was also included where applicable. These survey data extend from pre-2000 to the present day. The data were available to view as single profiles using the EA SANDS software, or as bulk spatial data provided for specific survey times from the CCO.

All of the bathymetric data were merged into a seamless bathymetry grid. Where possible the latest LIDAR data were used in preference, followed by the CCO bathymetry, LIDAR data and then the SeaZone data. Prioritising the datasets in this way ensured that the best quality data were used where they were available. The data were also inspected, once merged, to ensure that the locations where datasets intersected did not contain steep changes in bathymetry, which would distort wave transformation and the nearshore structures were included. The refined merged bathymetry dataset is shown in Figure J-4.

Boundary conditions

The calibrated wave model was used to calculate the extreme wave conditions at Jaywick. The model was run with two boundary conditions; extreme sea-levels and design wind conditions. These boundary conditions are described in the following sub-sections.

Extreme sea-levels

The wave transformation model also required a sea-level grid. The inclusion of sea-level within a wave transformation model is important because it establishes the depth of water that the waves will travel through, a key parameter that affects wave properties. Extreme sea-levels were extracted from the Environment Agency/Defra R&D Coastal Flood Boundary Data Study (CFB)[21]. Extreme sea-levels from this dataset take into account storm surge as well as astronomical tide levels. The extreme sea-levels of Jaywick are displayed in Table J-1.

[21] Environment Agency/DEFRA (2011), Project SC060064; Coastal Flood Boundary Conditions for UK Mainland and Islands, JBA Consulting and Royal Haskoning.

Table J-1. Extreme sea-levels of Jaywick

Return Period (year)	Year	Jaywick (mAOD)
1	2014	3.14
2		3.25
5		3.40
10		3.53
20		3.63
25		3.67
50		3.77
75		3.84
100		3.88
150		3.94
200		3.99
250		4.02
300		4.03
500		4.11
1,000		4.20
10,000		4.43
200	2023	4.02
1,000		4.23
200	2055	4.29
1,000		4.50
200	2112	5.05
1,000		5.26

Climate change for sea-levels

Climate change estimates have been based on the current guidance supporting the NPPF 'Climate Change for Planners' produced by the Environment Agency in September 2013. For this study, the medium emissions scenario has been considered, using the 95th percentile confidence rating. This gives a projected sea-level rise of 1.06m by the year 2112 from 2014. Extreme sea-levels and the adjustment for climate change are displayed in Table J-2.

Table J-2. Climate change water level increases at Jaywick

Year	Climate change (m)
2023	0.03
2055	0.30
2112	1.06

Extreme wind analysis

The variable required for the wave transformation model was wind speed and direction data. These data were required to ensure realistic wave generation and propagation within the model domain. The wind conditions were obtained from the hindcast wave model dataset. For the ensemble model simulations, a range of wind speed and direction conditions were used, as described in Section J.3.4. The calculations of wind speed return periods were completed using R-Code and is described below.

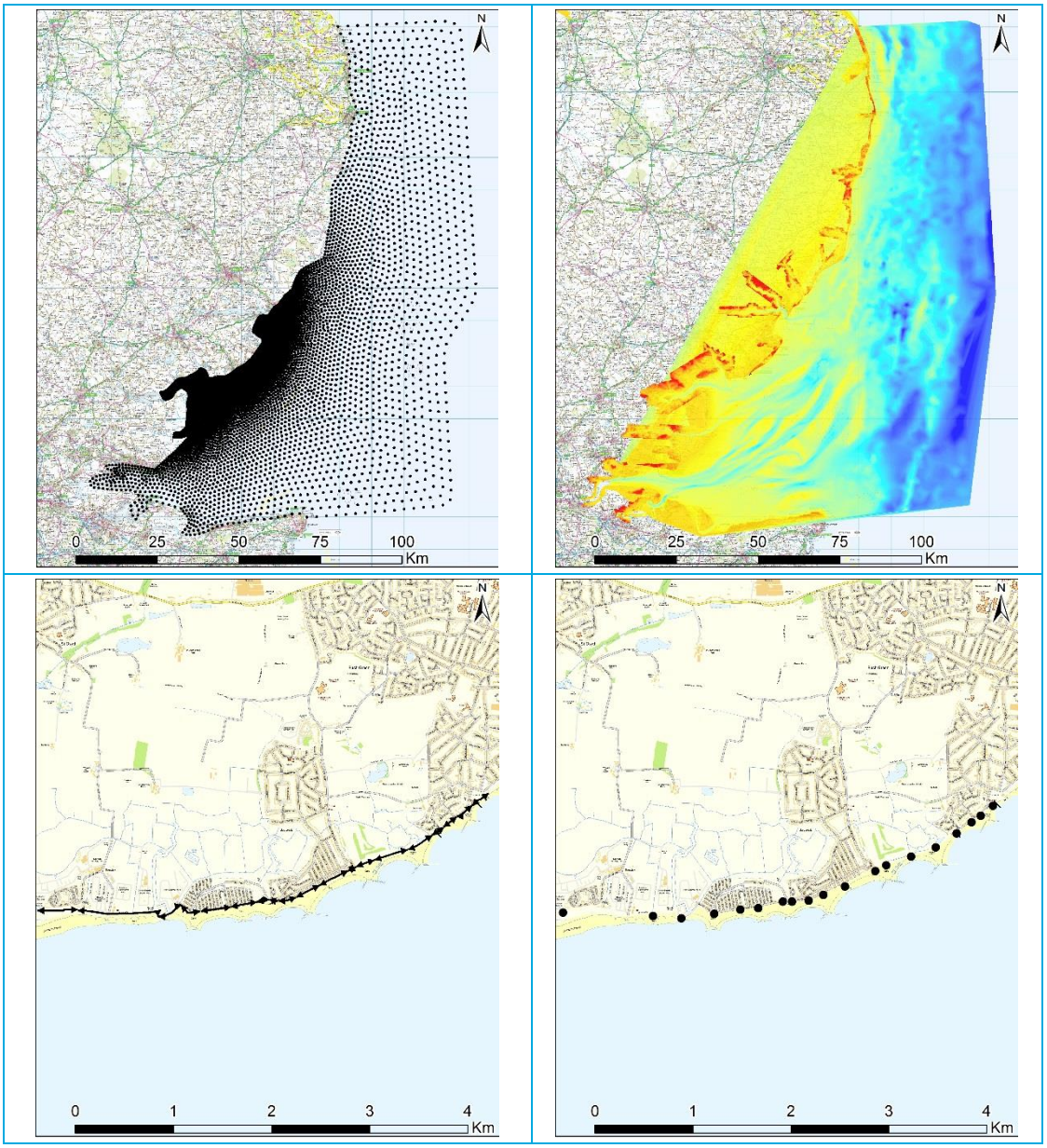

Figure J-4: SWAN model data, showing: Top left: Computational nodes. Top right: model bathymetry Bottom left: Schematised defences location. Bottom right: Wave reporting point at Jaywick (Contains Ordnance Survey data © Crown copyright and database right 2015)

R-Code

Generation of wind speed return periods requires extreme value marginal analysis. A typical extreme value marginal analysis uses a Peaks Over Threshold (POT) approach[22]. This involves defining a high threshold **u**, fitting a Generalised Pareto Distribution (GPD) with two parameters σ_u and **ξ** to all the observations that exceed the threshold, and estimating the rate of threshold exceedance **λ**. The fitted GPD distribution, together with the rate of threshold exceedance, implies a Generalised Extreme Value (GEV) distribution for the annual maximum observation, whose parameters are a function of (**u, σ_u, ξ, λ**), see for example Eastoe and Tawn (2010)[23]. This induced GEV distribution is then used to estimate the wind height for a range of return periods.

The POT method requires a long time series of complete data for the analysis. Wave Watch III hindcast wind data is available at sites around the UK for 3-hourly intervals between January 1980 and December 2014 and therefore is of suitable length and completeness for the POT analysis. A threshold was applied to the wind speed data series and the peak wind speed of events above the threshold were used to fit the GPD. Storm duration of 50 hours was used to identify occurrences above the threshold that were due to the same storm event.

Several appropriate thresholds were tested to ensure the best performance of modelled fit. The performance of the modelled fit was tested by comparing the recorded wind speed with those predicted by the modelled fit (0.70) as shown in Figure J-5. This comparison includes the wind speed generated by the upper and lower 95% confidence bounds of the GPD. A perfect fit would show an exact 1:1 relationship on the probability and quantile plots whilst the density and return level plots would show good agreement between the plotted lines and points respectively.

The return level plot in Figure J-5 also shows the greater uncertainty in estimated wind speed for the higher return periods and reflects the smaller number of high return period wind events in the wind record. To some extent, this is a result of the length of the wind record, which is 30 years, however by definition the high return period events are the least frequent and therefore will always be associated with greater uncertainty.

Since locations around the coastline are not equally vulnerable to wind from all compass directions, wind direction must be considered as a covariate in the POT analysis. Thus, the return period of wind speed derived for a particular direction is a function of both the probability of the wind speed occurring and the probability of the wind from a particular direction. The data was therefore split into relevant direction sectors and a probability distribution of wind speed was generated for each sector.

The estimated extreme wind speeds per return period are presented in Table J-3 by direction sector. Note, only the NE, SE, S and SW sectors were derived for the wind speed. This data was used in the Joint Probability analysis (Section J-5).

Table J-3. The estimated extreme wind speeds (m/s) per return period by direction sector

Return Period	SW	NE	SE	S
1	15.93	12.41	11.78	15.97
2	17.19	13.32	12.79	17.02
5	18.64	14.29	13.93	18.12
10	19.60	14.88	14.66	18.78
20	20.45	15.37	15.30	19.33
25	20.71	15.51	15.48	19.48
30	20.91	15.61	15.63	19.60
50	21.44	15.89	16.01	19.90
75	21.82	16.08	16.28	20.11
100	22.08	16.20	16.46	20.24
150	22.43	16.36	16.70	20.41
200	22.66	16.46	16.86	20.52
250	22.83	16.54	16.97	20.60
400	23.17	16.68	17.20	20.76

[22] Coles. S, (2001) An Introduction to Statistical Modeling of Extreme Values, Springer-Verlag, ISBN 1852334592.
[23] Eastoe, E. F and Tawn, J. A. (2010). Statistical models for over-dispersion in the frequency of peaks over threshold data from UK flow series. Water Resources Research, 46, W02510, doi:10.1029/2009WR007757.

Return Period	SW	NE	SE	S
500	23.32	16.74	17.30	20.82
1,000	23.76	16.91	17.58	21.00
10,000	24.89	17.29	18.28	21.39

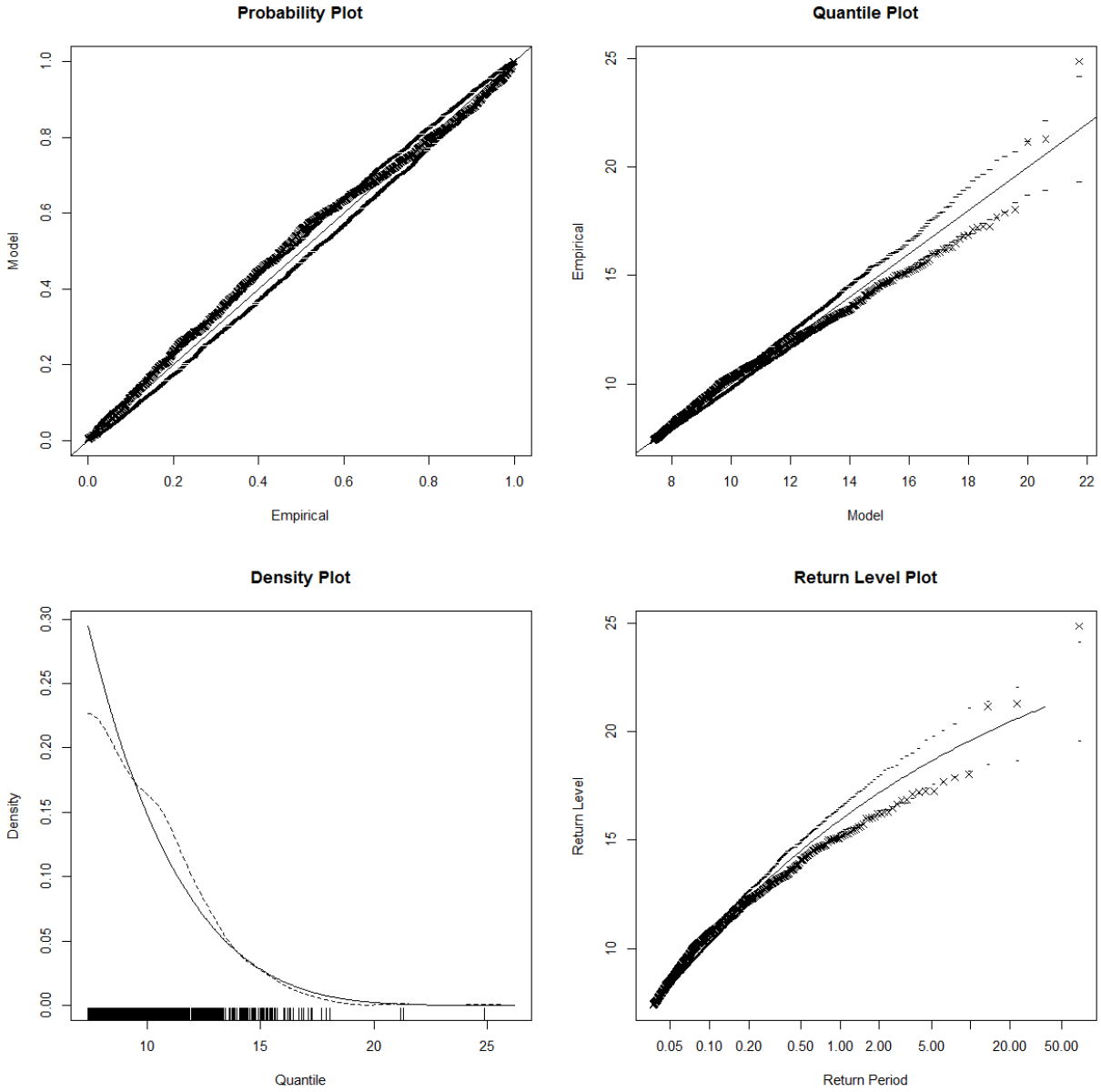

Figure J-5: Modelled Generalised Pareto Distribution of south westerly wind speed compared with WWIII hindcast data

J.3.4 Joint probability

A joint probability analysis was undertaken to consider the likelihood of significant winds and water levels coinciding during an extreme event. The level of dependence between wind and water levels was calculated using the industry standard Department of the Environment, Food and Rural Affairs (Defra) desk-based method[24]. A dependence value x (chi), of 0.15 was applied based on the surge vs wind speed dependence estimates presented in Defra technical report on dependence mapping[25], as shown in Figure J-6. Four different wind directions for thirteen different extreme water level conditions for the Jaywick, resulting in a total of 428 different wave models were simulated, each representing a potential return period between 5 and 200 years with climate change to the year 2112.

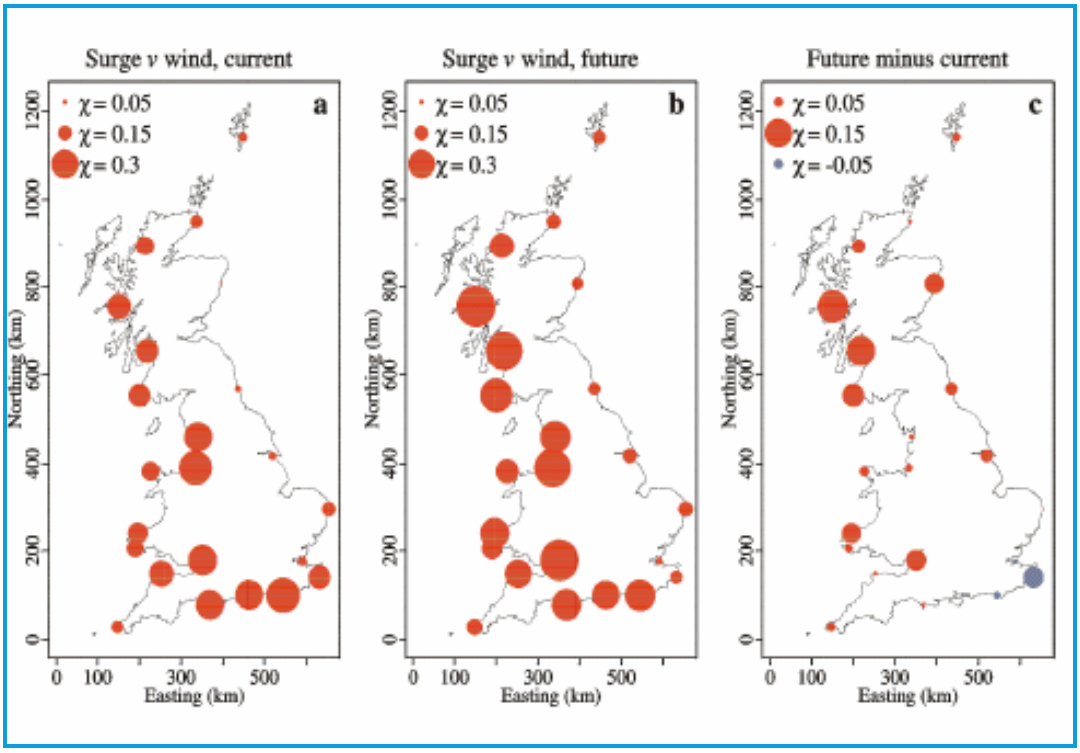

Figure J-6: Dependence of surge vs wind conditions (Defra 2005)

J.3.5 Wave overtopping

Approach and tolerable thresholds

The complexity of the physical processes leading to wave overtopping introduces a high degree of uncertainty into its quantification. As a result, the overtopping caused by individual waves is not typically calculated; instead the average overtopping rate for a particular sea-state is estimated using empirical or physical models. An example is the Neural Network tool, which was used for this study. This empirical-based model is described in the industry standard EurOtop[26] manual as the most suitable methodology for evaluating wave overtopping for composite defences such as seawall structures and armour. Even so, as with all calculation approaches, the Neural Network tool has limitations. Estimates are given based on a dataset of small-scale physical model tests which are affected by model and scale effects, the accuracy of measurement equipment and wave generation techniques. There is also the potential for limited data for particular schematisations, for example overtopping across wide (say 30.00m wide) beaches, as few model tests are available within the database. As a result, it is important that the results of the Neural Network are used with a degree of engineering judgement and caution.

[24] Defra (2005) Use of Joint Probability Methods in Flood Management: A Guide to Best Practice, Defra and the Environment Agency, March 2005, including associated spreadsheet.

[25] Defra (2005) Joint Probability: Dependence Mapping and Best Practice: Technical report on dependence mapping R&D Technical Report FD2308/TR1 March 2005

[26] EurOtop (2010) "Wave Overtopping of Sea Defence and Related Structures: Assessment Manual", Overtopping Course Edition, November 2010. HR Wallingford.

The Neural Network tool can be applied to different beach profiles, the geometric properties of which are characterised using 15 parameters including: crest height (Rc); armour height (Ac); armour width (Gc); berm elevation (hb); berm width (B); upper slope (α_u); lower slope (α_d); and roughness (γ_f) (see Figure J-7).

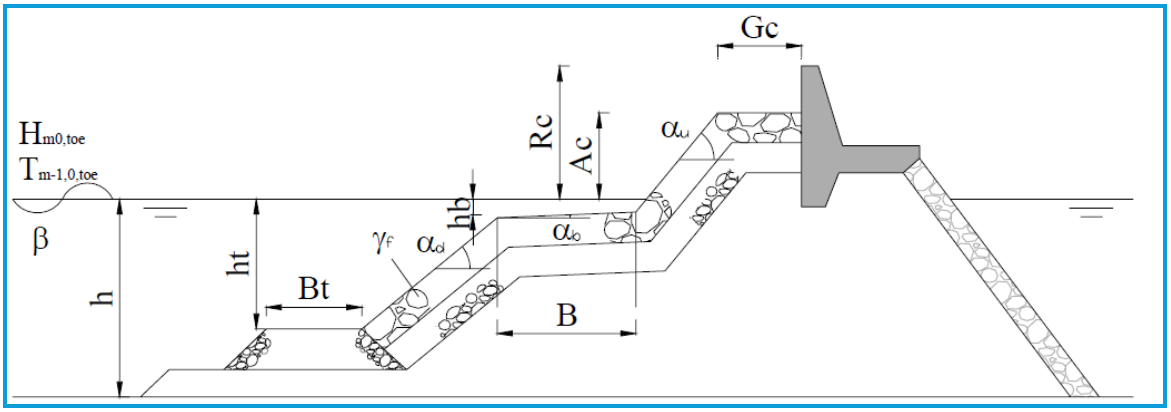

Figure J-7: Schematisations of a typical beach profile for analysis using the Neural Network overtopping tool

Using the Neural Network model, the average rate of overtopping can be calculated for a beach or defence cross-section. These can then be related to guidance given in the EurOtop manual which relates hazardous situations to overtopping rates and volumes. The tolerable limits for pedestrians and vehicles are given in Table J-4 and Table J-5 respectively. The limits for damage to the defences by overtopping discharge is presented in Table J-6.

Table J-4. Limits for overtopping for pedestrians (source: EurOtop).

Hazard type and reason	Mean discharge Q (l/s/m)	Max volume Vmax (l/m)
Trained staff, well shod and protected, expecting to get wet, overtopping flows at lower level only, no falling jet, low danger of fall from walkway.	1-10	500 at low level
Aware pedestrian, clear view of sea, not easily upset or frightened, able to tolerate getting wet, wider walkway.	0.1	20-50 at high level or velocity

Table J-5. Limits for overtopping for vehicles (source: EurOtop).

Hazard type and reason	Mean discharge Q (l/s/m)	Max volume Vmax (L/m)
Driving at low speed, overtopping by pulsating flows at low flow depths, no falling jets, vehicle not immersed.	10 - 50[27]	100 – 1,000
Driving at moderate or high speed, impulsive overtopping giving falling or high velocity jets.	0.01 – 0.05[28]	5 – 50 at high level or velocity

Table J-6. Limits for overtopping for property and damage to the defence (source: EurOtop).

Hazard type and reason	Mean discharge Q (l/s/m)
Damage to building structural elements	1[29]
Damage to equipment set back 5-10m	0.4[30]
No damage to embankment/seawalls if crest and rear slope are well protected	50-200
No damage to embankment / seawall crest and rear face of grass covered embankment of clay	1-10

[27] Note: These limits relate to overtopping defined at highways.
[28] Note: These limits relate to overtopping defined at the defence, assumes the highway is immediately behind
[29] Note: This limit relates to the effective overtopping defined at the building
[30] Note; This limit relate to overtopping defined at the defence

Hazard type and reason	Mean discharge Q (l/s/m)
Damage to paved or armoured promenade behind a seawall	200
Damage to grassed or lightly protected promenade	50

Overtopping model setup

The Jaywick coastal defence is a composite of a number of sections, varying in form and material. The defence was divided into 19 sections and schematised using the 15 Neural Network parameters. The profiles schematisations were based on field survey supplied by the Environment Agency. An example of a schematised defence section is shown in Figure J-8.

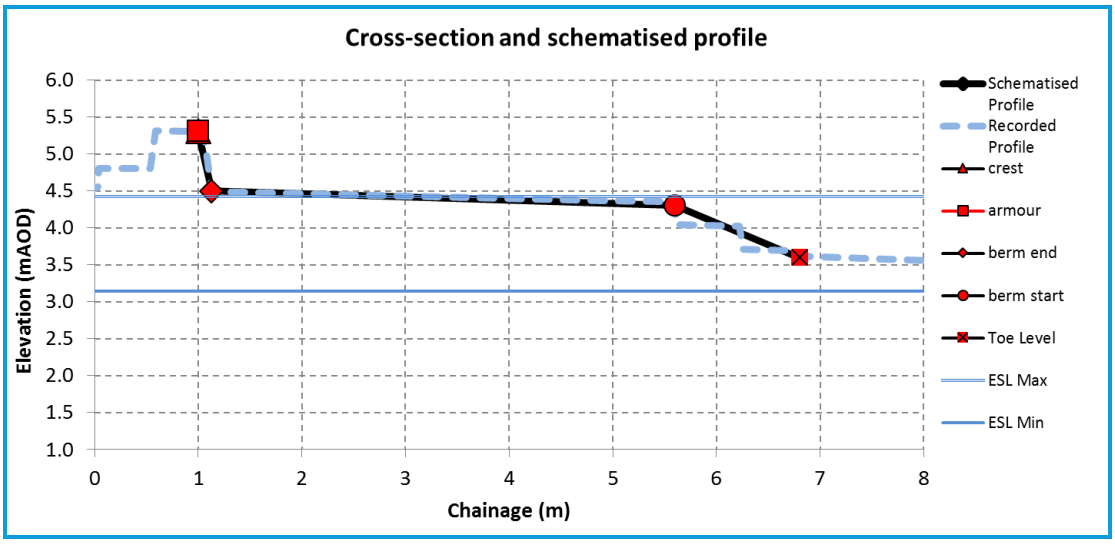

Figure J-8: Defence profile schematised using Neural Network.

Overtopping model results

The overtopping modelling was performed for the 19 defence sections (Figure J-9) for a 428 of joint probability scenarios, ranging from 5 to 1,000-year return periods under present day conditions. The rate of overtopping for each worst-case return period simulation is shown in Table J-7. These range from 0.00 to 2.34 l/s/m for a 5-year event, and 0.00 to 78.26 l/s/m for the 1,000-year event. Under climate change conditions for the 200 and 1,000-year. The rate of overtopping for each worst-case return period simulation is shown in Table J-8. These range from 0.00 to 54.61 l/s/m for a 200cc (2023)-year event, and 0.00 to greater than 115.00 l/s/m for the 1,000cc (2112)-year event.

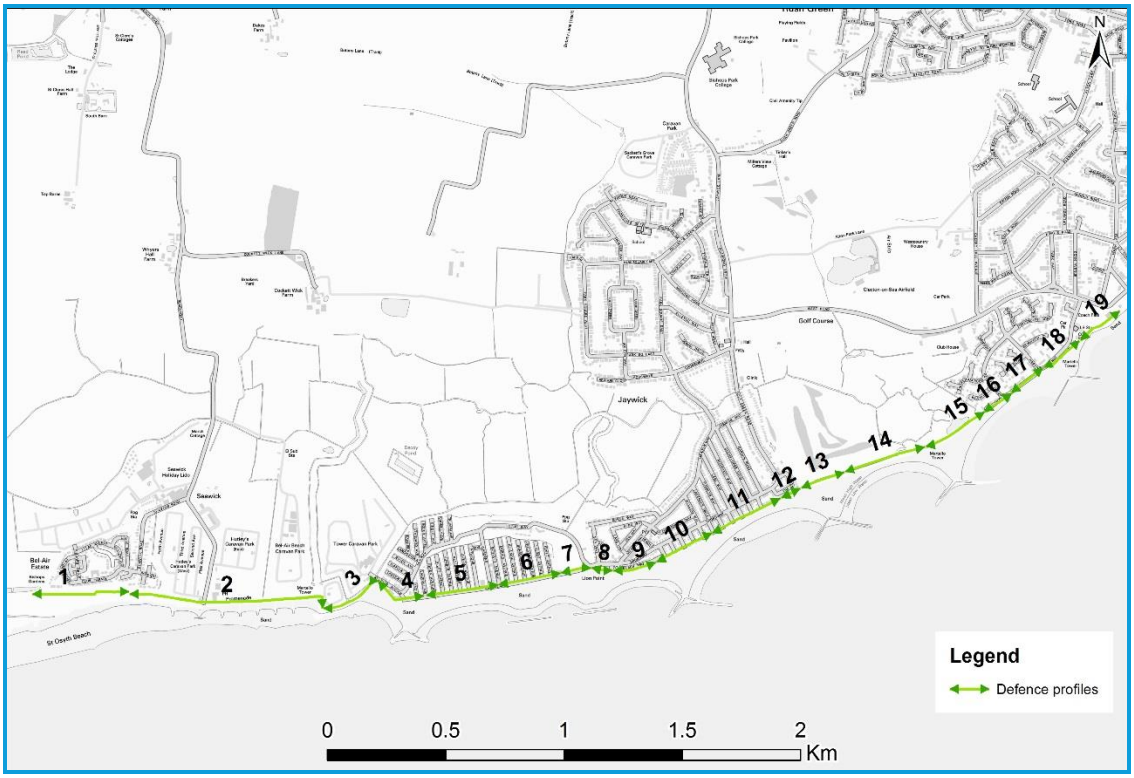

Figure J-9 Defence locations for the overtopping calculations (Contains Ordnance Survey data © Crown copyright and database right 2015)

Table J-7. The maximum overtopping ranging from 5 to 1,000-year return periods under present day conditions

Defence profile	Overtopping rates at l/s/m						
	Return period (year)						
-	5	20	25	50	75	200	1,000
1	0.00	0.00	0.00	0.00	0.13	1.14	12.66
2	0.00	0.00	0.00	0.00	0.00	4.28	33.52
3	2.34	9.74	12.56	25.07	35.50	62.56	73.94
4	0.00	0.00	0.00	0.00	0.00	0.00	0.02
5	0.00	0.00	0.00	0.00	0.00	0.00	0.00
6	0.00	0.00	0.00	0.00	0.00	0.00	0.09
7	0.00	0.00	0.00	0.00	0.00	0.00	0.00
8	0.00	0.00	0.00	0.00	0.00	0.00	0.00
9	0.00	0.00	0.00	0.00	0.00	0.00	0.00
10	0.00	0.00	0.00	0.00	0.00	0.00	0.01
11	0.00	0.01	0.02	0.32	1.28	7.36	28.58
12	0.00	0.00	0.00	0.00	0.00	0.00	0.00
13	0.00	0.00	0.00	0.00	0.00	0.00	0.01
14	0.00	0.11	0.23	1.30	3.62	19.50	78.26
15	0.00	0.00	0.00	0.00	0.00	0.00	0.35
16	0.00	0.00	0.00	0.00	0.00	0.00	12.91
17	0.00	0.00	0.00	0.00	0.00	0.00	0.09
18	0.00	0.00	0.00	0.00	0.00	0.00	0.00
19	0.00	0.02	0.03	0.07	0.13	0.39	1.60

Table J-8. The maximum overtopping ranging from 200cc (2023) to 1,000 (2112)-year return periods under climate change conditions

Defence profile	Overtopping rates at l/s/m					
	Return period (year)					
-	200cc (2023)	200cc (2055)	200cc (2112)	1,000cc (2023)	1,000cc (2055)	1,000cc (2112)
1	1.62	22.39	69.35	16.16	63.90	70.52
2	6.10	56.31	79.89	41.66	114.50	>115.00*
3	54.61	68.99	>69.00*	80.05	92.39	>93.00*
4	0.00	0.08	1.56	0.03	1.52	1.48
5	0.00	0.03	17.42	0.01	1.12	17.53
6	0.00	0.37	27.68	0.16	6.63	27.61
7	0.00	0.03	15.68	0.01	1.25	13.78
8	0.00	0.00	30.06	0.00	0.08	31.47
9	0.00	0.00	7.90	0.00	0.02	8.58
10	0.00	0.03	4.44	0.01	0.78	4.02
11	8.82	32.89	43.44	32.45	45.77	45.91
12	0.00	0.00	23.69	0.00	0.07	27.93
13	0.00	0.12	9.81	0.02	11.88	>12.00*
14	24.79	62.52	109.30	63.53	81.69	111.70
15	0.00	1.86	3.87	0.63	11.12	>12.00*
16	0.00	8.85	0.00	15.00	>15.00*	>15.00*
17	0.00	0.17	37.07	0.13	3.66	42.65
18	0.00	0.00	16.68	0.00	0.00	19.10
19	0.44	1.38	14.42	1.82	5.16	17.02

* For these conditions the Neural Network is predicting high overtopping, which is capped as the parameters exceeding the calculation limits.

J.3.6 Overtopping calculations conclusion

The overtopping at Jaywick varies greatly along the coastal frontage. This is mainly due to the construction of the near shore breakwater and groynes. These features have retained sediment on the landward side of the structure and resulted in the growth of salients. The development of salients has increased the beach width and has improved the coastal protection immediately behind them.

J.4 Breach modelling

The following three breaching locations were identified for the study:

- Breach A: soft estuarine defence in Colne Point and Point Clear
- Breach B: soft coastal defence n Seawick to Colne Point (Lee-over-Sands)
- Breach C: hard defence wall in Brooklands

These locations are illustrated in Figure J-10.

These breach locations are the same as those modelled in the 2008 SFRA. They were chosen at that time based on the condition of the sea defences, and where ground levels behind the defences were lowest.

The following scenarios were modelled for each breach location:

- Scenario One: Tide level equivalent to flood defence crest height (peak modelled tide level for location A: 4.92 mAODN, peak modelled tide level for location B and C: 4.71 mAODN)
- Scenario Two: Tide level equivalent to Flood Warning return period threshold (peak modelled tide level: 3.40 mAODN)
- Scenario Three: Tide level equivalent to Severe Flood Warning return period threshold (peak modelled tide level: 3.7 mAODN)

The breaches have been modelled individually (i.e. multiple breaches have been assumed not to occur).

For each breach the model was run over three tidal cycles with the peak level occurring in the second breach, remaining open for the remainder of the simulation (assumes the breach has not been repaired). This allows any potential overtopping to occur in the first tide cycle as well as allowing water to enter through the open breach in the third tide cycle.

Breaches were modelled to occur immediately before the peak tide. The breach width adopted for the earth embankments (locations A and B) was 50m while the breach width for the flood wall at location C was 20m. Further details of the modelled breaches are provided in Table J-9.

Figure J-10 Defence breach locations

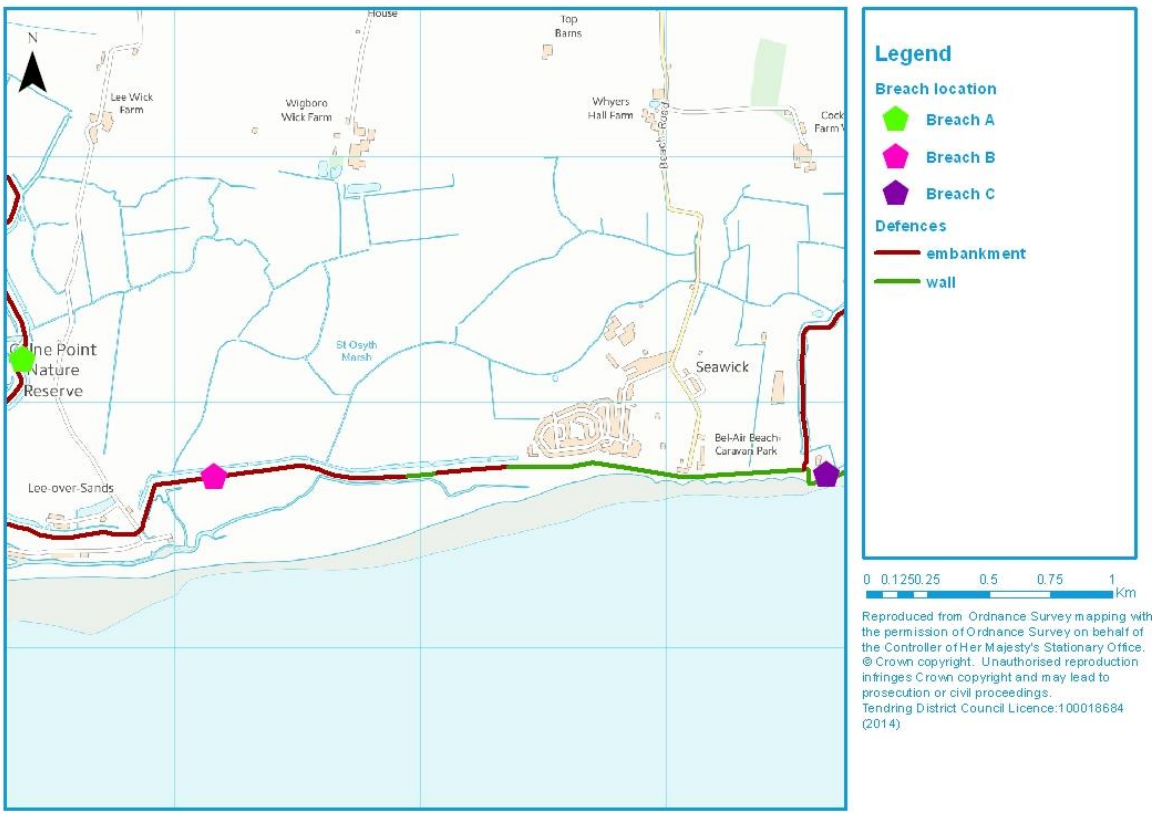

Table J-9.Breach model parameters

Breach location	Easting	Northing	Breach width (m)	Breach Invert (m AOD)
A	610383	213181	50	1.33
B	611161	212701	50	1.11
C	613654	212711	20	1.75